

## AN ORBIT FOR THE WC7 WOLF-RAYET BINARY HD 97152—COMPARISON WITH THE SINGLE-LINE WC7 STAR HD 156385<sup>1</sup>

ANTHONY B. DAVIS AND ANTHONY F. J. MOFFAT  
 Département de physique, Université de Montréal

AND

VIRPI S. NIEMELA<sup>2</sup>  
 Instituto de Astronomía y Física del Espacio, and Instituto Argentino de Radioastronomía,  
 Villa Elisa, Buenos Aires

Received 1980 June 3; accepted 1980 July 29

### ABSTRACT

A spectroscopic comparison of the two stars yields a spectral type for HD 97152 of WC7 + O7 V. Radial velocity measurements of this star indicate a double-line circular orbit with period  $7^{\text{d}}886 \pm 0^{\text{d}}003$  and masses  $M(W) \sin^3 i = 3.6 \pm 0.3 M_{\odot}$  and  $M(O) \sin^3 i = 6.1 \pm 0.5 M_{\odot}$ . The mass ratio,  $M(W)/M(O) = 0.59 \pm 0.02$ , falls in the range of other known galactic WR + OB binaries. Intermediate-band photoelectric photometry shows low-amplitude, sinusoidal magnitude variations with the same period for a filter which straddles the strong emission feature at 4650 Å whose Doppler motion alone can explain the magnitude variation. The continuum is constant to within  $\pm 0.005$  mag. Taking  $M(O7 V) = 29 M_{\odot}$ , we get an orbital inclination of  $36^{\circ}5$  and  $M(W) = 17.5 M_{\odot}$ , like the minimum mass for the WC8 component of  $\gamma^2$  Velorum. Significant radial velocity variations in HD 156385 are not detected.

*Subject headings:* stars: binaries — stars: individual — stars: Wolf-Rayet

### I. INTRODUCTION

Our present knowledge of Wolf-Rayet (WR) star masses is based exclusively on an incomplete sample of 12 galactic double-line systems brighter than  $v = 11$  mag (Moffat and Seggewiss 1980). Of these, only four are of the carbon sequence, ranging little in spectral subclass, from WC6-7 to WC8, each with a massive O-type companion. While several *single-line* binary WN stars are known, there are no such objects with a WC spectrum. The double-line WC7 + OB star HD 97152 (= MR 36 in the catalog of Roberts 1962), is one of the four WC binaries; in this paper, we present detailed spectroscopic and photometric data which lead to estimates of the masses of the WR and OB components.

HD 97512 is located  $\sim 3^{\circ}$  from the Great Carina Nebula, at the galactic coordinates  $l = 290^{\circ}95$ ,  $b = -0^{\circ}49$  and equatorial coordinates (2000):  $\alpha = 11^{\text{h}}10^{\text{m}}4^{\text{s}}0$ ,  $\delta = -60^{\circ}58'46''$ . With intermediate-band, visual continuum magnitude  $v = 8.25$  (Smith 1968*b*), it is the 16th brightest WR star in the sky. With color index  $b - v = 0.06$  it suffers only  $E_{b-v} = 0.20$  mag of extinction, despite its moderately large (preliminary) distance, 5.8 kpc (Smith 1968*c*). It is not a member of an open cluster or any obvious OB association, nor is it associated with any visible H II ring.

<sup>1</sup> Based partly on observations collected at the European Southern Observatory.

<sup>2</sup> Visiting Astronomer, Cerro Tololo Inter-American Observatory which is supported by the National Science Foundation under contract No. AST 78-27879; Member of Carrera del Investigador, Comision de Investigaciones Cientificas, Provincia de Buenos Aires, Argentina.

### II. DATA ACQUISITION

In order to study the light variations, photoelectric photometry was obtained by A.F.J.M. on 29 nights, spanning a total interval of 37 days (1975 February 4–March 13) using the single-channel photometer of the Bochum University's 61 cm telescope on La Silla, Chile. Observations were made alternately with two comparison stars: HD 96970 and HD 96829, of spectral types AI V and B3 III, respectively. As it turned out, the B3 star was a slow variable (Moffat 1977) and was not used in the final reduction. The A star, which has constant magnitude, is situated  $9'$  NW of the WR star. Three filters were used with central wavelengths and full widths at half-intensity, respectively, of 3635, 70 Å; 4680, 130 Å; 5170, 190 Å. The first and last filters were chosen to coincide with as emission-free parts of the spectrum as possible at widely separated wavelengths, while the second filter contains the strongest optical emission feature due to C III(IV)4650 and He II 4685. Typical integration times per filter observation were 30–60 s through an 18" diameter diaphragm. A journal of photometric observations is presented in Table 1. Subtracting out the slow secular variations of HD 96829, the standard deviations for  $m(96829) - m(96970)$  in the three filters are 0.011, 0.007 and 0.008 mag, respectively. These will serve as a basis for discussing the reality of the variations of  $m(97152) - m(96970)$  in § IV.

In order to obtain a radial velocity orbit and to look for other possible phase-dependent changes in the lines, we have two sources of spectra:

- 1) A series of 15 Cassegrain spectrograms obtained by

TABLE 1  
PHOTOELECTRIC PHOTOMETRY OF  $\Delta m = m(\text{HD } 97152) - m(\text{HD } 96970)$   
AND THE CORRESPONDING PHOTOMETRIC VELOCITIES FROM THE  
SHIFT OF THE EMISSION FEATURE IN THE  $\lambda 4680$  FILTER<sup>a</sup>

| JD-<br>2 440 000 | phase  | $\Delta m(3635\text{\AA})$ | $\Delta m(4680\text{\AA})$ | $\Delta m(5170\text{\AA})$ | RV(4680)<br>* |
|------------------|--------|----------------------------|----------------------------|----------------------------|---------------|
| 2447.8558        | 0.0365 | 0.074                      | 0.040                      | -0.729                     | - 50          |
| 2448.7440        | 0.1491 | 0.084                      | 0.024                      | -0.741                     | +160          |
| 2449.8094        | 0.2842 | 0.058                      | 0.028                      | -0.742                     | +105          |
| 2451.7878        | 0.5351 | 0.060                      | 0.047                      | -0.741                     | -135          |
| 2452.7930        | 0.6626 | 0.060                      | 0.034                      | -0.734                     | + 25          |
| 2453.7947        | 0.7896 | 0.066                      | 0.050                      | -0.738                     | -169          |
| 2454.8130        | 0.9187 | 0.073                      | 0.049                      | -0.739                     | -158          |
| 2455.8074        | 0.0448 | 0.058                      | 0.040                      | -0.738                     | - 50          |
| 2456.7944        | 0.1700 | 0.039                      | 0.024                      | -0.743                     | +160          |
| 2457.8156        | 0.2995 | 0.067                      | 0.022                      | -0.735                     | +188          |
| 2458.7991        | 0.4242 | 0.054                      | 0.021                      | -0.746                     | +202          |
| 2459.8253        | 0.5543 | 0.058                      | 0.040                      | -0.745                     | - 50          |
| 2460.7995        | 0.6779 | 0.062                      | 0.042                      | -0.749                     | - 75          |
| 2461.7686        | 0.8007 | 0.067                      | 0.048                      | -0.736                     | -146          |
| 2462.7007        | 0.9189 | 0.060                      | 0.046                      | -0.756                     | -123          |
| 2463.7450        | 0.0514 | 0.050                      | 0.029                      | -0.738                     | + 92          |
| 2464.6612        | 0.1675 | 0.060                      | 0.029                      | -0.737                     | + 92          |
| 2465.8022        | 0.3122 | 0.084                      | 0.024                      | -0.737                     | +160          |
| 2466.7665        | 0.4345 | 0.077                      | 0.023                      | -0.743                     | +174          |
| 2467.8460        | 0.5714 | 0.088                      | 0.036                      | -0.737                     | 0             |
| 2468.8391        | 0.6973 | 0.064                      | 0.044                      | -0.739                     | - 99          |
| 2469.8456        | 0.8249 | 0.074                      | 0.039                      | -0.742                     | - 37          |
| 2470.8088        | 0.9471 | 0.072                      | 0.047                      | -0.737                     | -135          |
| 2471.7898        | 0.0715 | 0.074                      | 0.021                      | -0.746                     | +202          |
| 2472.7653        | 0.1952 | 0.079                      | 0.031                      | -0.736                     | + 65          |
| 2474.7059        | 0.4413 | 0.056                      | 0.037                      | -0.741                     | - 12          |
| 2478.7662        | 0.9561 | 0.066                      | 0.046                      | -0.747                     | -123          |
| 2482.7781        | 0.4649 | 0.042                      | 0.026                      | -0.743                     | +132          |
| 2484.7784        | 0.7185 | 0.060                      | 0.044                      | -0.742                     | - 99          |

\* Last column  $\text{km s}^{-1}$

<sup>a</sup>The phase ephemerides are calculated using the final elements in Table 7.

V.S.N. at CTIO using moderate dispersion. They are spread over a 2 year interval from 1975 March to 1977 March and never cover more than a five night span for a given run.

2) A series of 16 coudé spectrograms obtained by A.F.J.M. at ESO. They cover an uninterrupted interval of 15 days from 1977 February 22 to March 9 (UT).

All spectra are  $\sim 0.5$  mm wide and were obtained by using a slit whose projection corresponds to the resolution of the detector. The exposure time for any given plate was in the range  $\sim 20 \pm 5$  minutes. Wavelength calibration is iron arc. A journal of spectroscopic observations is presented in Table 2 which includes four spectra obtained of HD 156385 = MR 69, a seventh mag single-line WC7 star of the same subclass as the WR component of HD 97152.

### III. SPECTRAL CLASSIFICATION AND DISTANCE

HD 97152 is listed with spectral class WC7 + BO V:: by Smith (1968a). The classification of WC stars follows mainly from the half-width of the C III(IV) 4650 emission complex, which is the strongest feature in the optical spectrum. We verify this for HD 97152 in Figure 1, which shows the typical intensity profile of this feature from one of the coudé plates. The arrow indicates a total width at

half-intensity maximum of  $30 \text{ \AA}$  ( $36 \text{ \AA}$  for HD 156385) which corresponds well with WC7 (Smith 1968a). Thus, we adopt an absolute magnitude for the WR component according to its spectral class:  $M_V(\text{WC7}) = -4.4 \pm 0.5$  mag (estimated s.d.) following the calibration of Smith (1973).

In order to classify the OB companion, we show in Figure 2 photographic density scans of HD 97152 and, with the same wavelength scale, of the single-line WC7 star HD 156385. The radial velocities of HD 156385 show no significant changes and support its possible single nature (cf. Table 3), although more plates are needed on a longer time base. Comparison of these two stars allows an easy distinction of the relatively narrow absorption lines in the OB companion of HD 97152 from the broad WR emission lines. The most important absorption lines identified are those of He I 4471 and He II 4541 whose intensity ratio ( $\sim 1.0$  here) is a good signature of the spectral subclass for O stars (Conti and Alschuler 1971). We adopt O7 here.

The absence of Si IV 4089 absorption does not necessarily imply low luminosity ( $V$ ) for the O7 star, since the spectrum is weakened by the WC7 continuum and He I 4143 is not evident either. Also, the presence of Si IV 4089 is uncertain due to the dip between two emission features

TABLE 2  
JOURNAL OF SPECTROSCOPIC OBSERVATIONS

| Plate            | JD-<br>2440000 | Emulsion<br>(b=baked) | Reciprocal<br>dispersion<br>( $\text{\AA}^{-1} \text{mm}^{-1}$ ) | Telescope |      |
|------------------|----------------|-----------------------|--|-----------|------|
| <u>HD 97152</u>  |                |                       |  |           |      |
| A4106            | 2472.900       | IIa0                  | 42   | 0.9m      | CTIO |
| A4111            | 2474.716       | IIa0b                 | "  | "         | "    |
| A4112            | 2474.792       | IIIaJb                | "  | "         | "    |
| A4116            | 2475.828       | "                     | "  | "         | "    |
| A4119            | 2476.790       | "                     | "  | "         | "    |
| A4123            | 2477.780       | "                     | 120  | "         | "    |
| A4424            | 2877.790       | "                     | 60   | "         | "    |
| A4428            | 2878.643       | IIa0                  | "  | "         | "    |
| A4433            | 2879.724       | IIIaJb                | "  | "         | "    |
| A4439            | 2880.735       | "                     | 42   | "         | "    |
| A4443            | 2881.663       | "                     | 60   | "         | "    |
| C4754            | 3143.816       | "                     | 38   | 1.5m      | "    |
| C4804            | 3201.793       | "                     | "  | "         | "    |
| C4810            | 3202.810       | "                     | "  | "         | "    |
| C4824            | 3203.719       | "                     | "  | "         | "    |
| <br>             |                |                       |  |           |      |
| F5014            | 3196.878       | IIa0b                 | 20   | 1.5m      | ESO  |
| F5023            | 3197.802       | "                     | "  | "         | "    |
| F5031            | 3198.846       | "                     | "  | "         | "    |
| F5036            | 3199.814       | "                     | "  | "         | "    |
| F5040            | 3200.787       | "                     | "  | "         | "    |
| F5044            | 3201.597       | "                     | "  | "         | "    |
| F5048            | 3202.606       | "                     | "  | "         | "    |
| F5053            | 3203.789       | "                     | "  | "         | "    |
| F5057            | 3204.640       | "                     | "  | "         | "    |
| F5060            | 3205.829       | "                     | "  | "         | "    |
| F5065            | 3206.810       | "                     | "  | "         | "    |
| F5069            | 3207.676       | "                     | "  | "         | "    |
| F5070            | 3208.640       | "                     | "  | "         | "    |
| F5077            | 3209.599       | "                     | "  | "         | "    |
| F5081            | 3210.581       | "                     | "  | "         | "    |
| F5086            | 3211.812       | "                     | "  | "         | "    |
| <br>             |                |                       |  |           |      |
| <u>HD 156385</u> |                |                       |  |           |      |
| G8113            | 3203.860       | IIa0b                 | 12   | 1.5m      | ESO  |
| G8247            | 3206.912       | "                     | "  | "         | "    |
| G8288            | 3209.906       | "                     | "  | "         | "    |
| G8314            | 3211.913       | "                     | "  | "         | "    |

at this wavelength, seen also in the single-line star HD 156385. An alternate way to arrive at an estimate of the luminosity class of the O7 star is to obtain its absolute luminosity and convert to luminosity class by using the calibration of Conti and Alschuler (1971). To do this, we assumed (1) that both WC7 stars have the same  $M_v$ , (2) that the ratio of the peak intensity of a given emission line above the continuum to the WR-continuum is (a) the same for both WC7 stars HD 97152 and HD 156385, or (b) inversely proportional to the line width, i.e., one assumes constant equivalent width, and (3) that these line ratios are not perturbed by O-star absorption lines at the positions chosen. The two lines for which it is least difficult to estimate the underlying continuum level are those of C III(IV) 4650 and C IV 4441. Because of its unexplained absorption feature in HD 156385, the latter is only used for consistency and dispersion evaluation.

Thus, for HD 97152 we find

$$M_v(\text{WC7}) - M_v(\text{O7}) = +0.2 \pm 0.4 \text{ mag} \quad (\text{a})$$

$$M_v(\text{WC7}) - M_v(\text{O7}) = +0.5 \pm 0.2 \text{ mag}, \quad (\text{b})$$

and with  $M_v(\text{WC7}) = -4.4 \pm 0.5$  we get

$$M_v(\text{O7}) = -4.6 \pm 0.6 \text{ mag} \quad (\text{a})$$

$$M_v(\text{O7}) = -4.9 \pm 0.5 \text{ mag}. \quad (\text{b})$$

Taking Smith's  $v$  magnitude to be essentially equal to the broad-band magnitude  $V$ , we finally arrive for either (a) or (b) at O7 V, for which Conti and Alschuler (1971) give  $M_v = -4.8$ .

The total absolute magnitude of HD 97152 is thus  $-5.3 \pm 0.5$  mag. Following Smith (1968c) we adopt  $E_{B-V} = 0.20 \pm 0.05$  mag which, after Turner (1980), leads

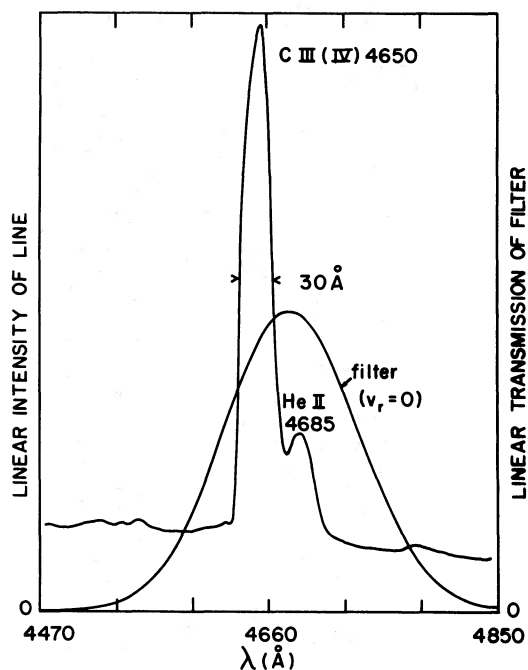


FIG. 1.—Intensity profile of C III(IV) 4650 Å and He II 4685 Å from plate F5086 and the adopted transmission profile of the 4680 filter.

to a total visual extinction  $A_v = 0.89 \pm 0.22$ . Therefore,  $v_0 = v - A_v = 7.36 \pm 0.22$  and  $v_0 - M_v = 12.6 \pm 0.55$  or a distance of  $3.3 (+1.0; -0.8)$  kpc. This places HD 97152 on the inner side of the Carina spiral arm (cf. Vogt and Moffat 1975) at a distance of 28 pc below the galactic plane, which is well within the mean ( $\sim 60$  pc) for extreme population I stars (Cruz-González *et al.* 1974).

#### IV. DATA REDUCTION

Heliocentric radial velocities for the least blended and generally strongest lines are listed in Table 3 (WC7 component of HD 97152 and single-line WC7 star HD 156385) and Table 4 (O7 V component of HD 97152). Originally, about twice as many emission lines, including those of higher and lower excitation potential as those listed, were measured, but as it turns out, they are noisy, vary as the stronger lines in the mean, and provide little new information.

The CTIO plates were measured for radial velocity by V.S.N. on a Grant measuring machine at the Instituto de Astronomía y Física del Espacio, Buenos Aires. The ESO plates were scanned by A.F.J.M. with the PDS at the David Dunlap Observatory, Toronto, and reduced in the photographic density mode using a method as described elsewhere (Moffat 1978). Generally, the latter set, being of higher dispersion, is generally more precise; a good test of this is reflected by the interstellar Ca II lines which can be expected intrinsically to have constant radial velocity. While the Cassegrain plates give a mean velocity for Ca II H and K of  $-11 \pm 10$  (s.d. for H or K)  $\text{km s}^{-1}$ , the coude plates yield  $-1.6 \pm 2.6$  (s.d.)  $\text{km s}^{-1}$ . No correction is

made for the marginally real difference in radial velocity between the two sets of plates.

The probability that the light variations of HD 97152 are intrinsic to the star was studied by comparing the observed scatter (s.d.) of  $m(\text{HD } 97152) - m(96970)$ : 0.012, 0.010, and 0.005 mag in the filters 3635, 4680, and 5170, respectively, with that of the corresponding differences of the two comparison stars as stated in § II. The only filter where a test is worthwhile is for 4680. The other s.d.'s are similar for the other two filters or even less for the WR star than the comparison stars in the case of the 5170 filter, probably a consequence of the fact that the secular variable HD 96829 may be slightly unstable. Using a Student's *F*-test with 28 degrees of freedom we find a  $\sim 3\%$  probability that the 4680 variations are due to chance. We conclude that HD 97152 is intrinsically variable in the line filter 4680 but constant, to within  $\pm 0.005$  in the continuum.

The most obvious possible source of intrinsic variation in the 4680 filter is a periodic Doppler shift of the strong emission feature C III(IV) 4650 (cf. § V) located near the steep part of the blue flank of the filter transmission curve. Using the known central wavelength of the filter (4680 Å) and adopting a Gaussian transmission profile with full width at half-maximum (130 Å; cf. Fig. 1), it is possible to reconstruct radial velocity changes of the 4650 feature by convolving the filter transmission function with the observed line + continuum intensity. For lack of more precise knowledge of the filter characteristics, we adopt radial velocity  $v = 0$  when the magnitude  $m \equiv m(\text{HD } 97152) - m(96970)$  is equal to its mean value  $m_0$  in the 4680 filter. Thus, we find for the range  $\Delta m = m - m_0 = \pm 0.015$ , the relation  $v = -128 (100 \Delta m) + 4.8 (100 \Delta m)^2$  with a precision of  $\pm 1 \text{ km s}^{-1}$ . The resulting velocities are listed in the last column of Table 1. With standard deviation 0.007 mag for  $\Delta m$ , on the basis of the comparison stars (possibly too pessimistic), the radial velocities have a corresponding precision of  $\lesssim 90 \text{ km s}^{-1}$ .

#### V. THE BINARY ORBIT

Before embarking on a detailed orbit analysis, we obtain a preliminary estimate of the period from the variable 4680 photometric data, which are very homogeneous and extend over a moderately long, continuous interval. The period search algorithm of Lafler and Kinman (1965) yields a period of  $P = 7^{\text{d}}84 \pm 0^{\text{d}}14$  with a single-wave per cycle. A period of  $15^{\text{d}}7$  would produce a double-wave but, as we shall see, is excluded by the radial velocity variations. A sine-wave fit gives a similar period  $P = 7^{\text{d}}90 \pm 0^{\text{d}}13$  and a residual rms dispersion of 0.006 mag, like that expected from the comparison stars.

The final value of the period was obtained from a preliminary orbit analysis of the best lines on the spectroscopic plates which have the most measures available. These are clearly C III(IV) 4650 *e* from the WR component and H $\delta$  *a* from the O star.

The following orbital parameters are available to fit the radial velocity data in the nonlinear least squares sense: period  $P$ , velocity semi-amplitude  $K$ , the time of passage

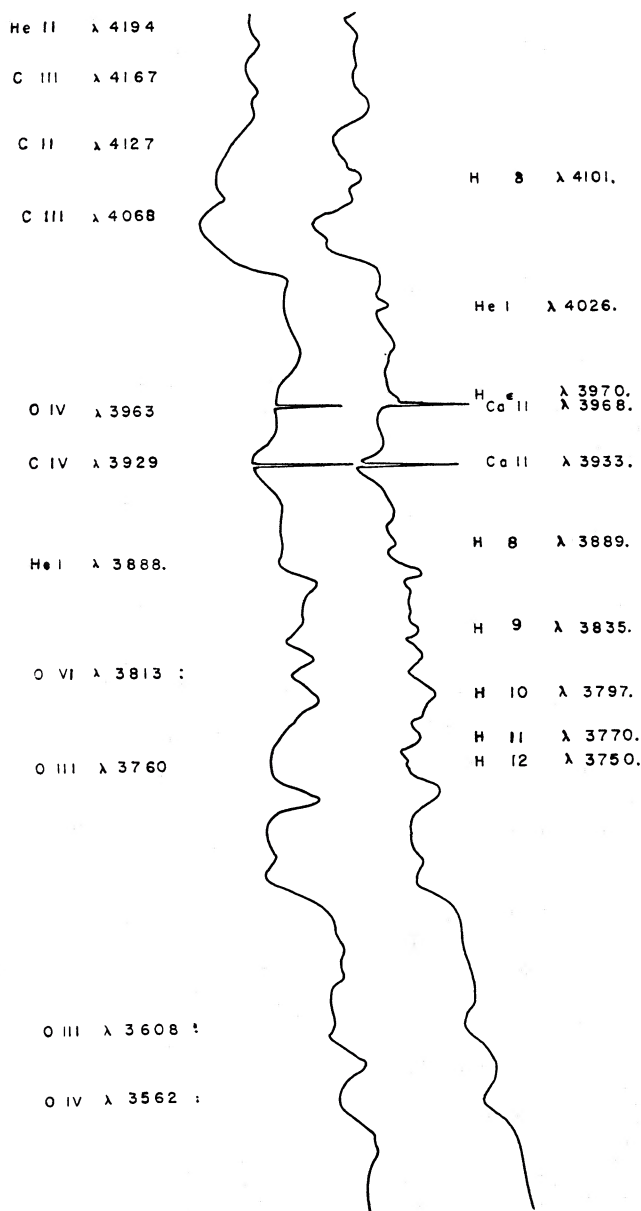


FIG. 2.—Smoothed photographic density scans of HD 156385 (WC7), plate G8247 and HD 97152 (WC7 + O7 V), plate F5086, reduced to the same scale. The principal emission features are identified above, the absorption below. Note the similarity of the WC7 components, although the former star has slightly wider emission lines and shows a curious red extension to the C iv 4441 Å feature (may be due to He I 4471), not seen in the latter.

through the systemic velocity (from negative to positive for the WR component)  $E$ , and one systemic velocity  $\gamma$  per set of spectrograms (thus allowing for any systematic difference between the radial velocities reduced from the CTIO plates on the one hand and the ESO plates on the other). The remaining spectroscopic elements, eccentricity  $e$ , and position of the periastron  $\omega$ , were allowed to vary only for the WR lines. Indeed, the absorption lines are compatible with zero eccentricity and for them  $e$  is constrained to zero. As seen in Table 4, the value of the eccentricity for some emission lines is small but

significantly different from zero. We assume that these values are intrinsically spurious, being due to the perturbation of the emitting WR envelope by the companion star. Thus, weighting the CTIO and the ESO data according to their respective dispersions, we obtain exactly the same period for C III(IV) 4650  $e$  as H $\delta$   $a$ :  $P = 7^d 886 \pm 0^d 003$ , which we adopt as final and  $e = 0$  as provisional.

Velocity curves according to the parameters in Table 5 and 6 for these two lines are shown in Figure 3. In Figure 4, we show the photometric velocities (cf.

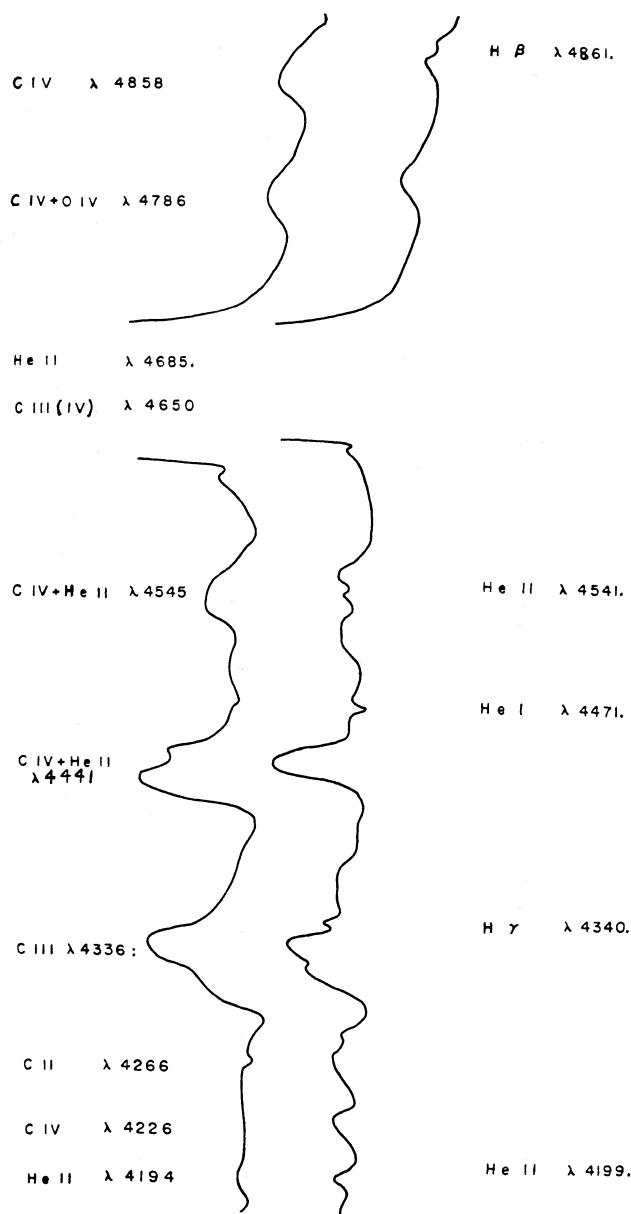


FIG. 2.—Continued

Table 1) with  $\gamma = +14 \text{ km s}^{-1}$  superposed on the curve for  $\text{C III}(\text{IV})e$  from Figure 3a. Despite the higher noise level, the photometric radial velocities are clearly phase-shifted relative to the spectroscopically determined radial velocities of the same emission feature. Presumably, this difference is due to the fact that one is not measuring the same part of the emission feature; the photometry is more sensitive to phase-dependent changes in the red flank of the line, while the spectroscopic velocities reflect overall line position. Nothing is obvious, however, in the photographic spectra. In any case, the amplitude of the photo-

metric radial velocities is the same; this implies that their variation is due to Doppler shift within the filter.

Using the above period, we made fits to the remaining WC7 emission line velocities; the results are given in Table 5. Among the emission lines, the  $\gamma$  velocities of CT10 and ESO are not significantly different. However, the phase-shifts and eccentricities are most different from zero for lines of lower excitation potential (EP). This is probably a consequence of the fact that these lines are formed farther out in the WR envelope where perturbations (e.g., streaming motions) caused by the companion

TABLE 3  
HELIOCENTRIC RADIAL VELOCITIES ( $\text{km s}^{-1}$ ) FOR THE BEST EMISSION  
LINES AND TWO P CYGNI ABSORPTION EDGES FOR THE WC7  
COMPONENT OF HD 97152 AND THE WC7 STAR HD 156385 AS  
WELL AS THE INTERSTELLAR ABSORPTION LINES OF Ca II<sup>a</sup>

| Ion:          | HeIa      | CIII(IV) <sup>a</sup> | CIII(IV) <sup>e</sup> | CIVe  | CIVe | HeIIe  | CaII-K | CaII-H |
|---------------|-----------|-----------------------|-----------------------|-------|------|--------|--------|--------|
| $\lambda_o$ : | 3888      | 4650                  | 4650                  | 4441  | 4786 | 4685   | 3933   | 3968   |
|               | .646      | -                     | -                     | -     | -    | .682   | .664   | .470   |
| Plate         | Phase     |                       |                       |       |      |        |        |        |
|               | HD 97152  |                       |                       |       |      |        |        |        |
| A4106         | 0.212     | -1225                 | -                     | -     | -    | -      | - 12   | - 22:  |
| A4111         | 0.443     | -                     | -                     | -     | - 29 | -      | -      | -      |
| A4112         | 0.452     | -                     | -                     | -     | - 40 | -      | -      | -      |
| A4116         | 0.584     | -1461                 | -                     | -     | -    | -      | + 1    | -      |
| A4119         | 0.706     | -1439                 | -                     | -     | -    | -      | - 5    | - 16   |
| A4123         | 0.831     | -1486                 | -1539                 | + 66  | -115 | -      | - 46   | 0      |
| A4424         | 0.832     | -1445                 | -1454                 | - 26  | -119 | -      | - 1    | + 11   |
| A4428         | 0.941     | -1586                 | -1517                 | -121  | -150 | -      | -272   | - 23   |
| A4433         | 0.078     | -1460                 | -1555                 | - 52  | -164 | -      | -211   | + 2    |
| A4439         | 0.206     | -                     | -                     | -     | -348 | -      | -      | -      |
| A4443         | 0.323     | -1534                 | -1395                 | +183  | + 8  | -      | + 52   | - 13   |
| C4754         | 0.288     | -1320                 | -1371                 | +234  | + 96 | -      | + 95   | - 18   |
| C4804         | 0.640     | -1456                 | -1443                 | - 49  | -197 | -      | -181   | - 15   |
| C4810         | 0.769     | -1468                 | -                     | -     | -177 | -      | -116   | - 25   |
| C4824         | 0.884     | -                     | -1623                 | +122  | -130 | -      | - 9    | -      |
| F5014         | 0.017     | -1414                 | -1458                 | +197  | - 52 | - 10   | +105:  | -3.4   |
| F5023         | 0.134     | -                     | -1504                 | +268  | + 5  | +130:  | +205   | -3.7   |
| F5031         | 0.266     | -1582                 | -1834                 | +244  | + 81 | +175   | +150   | -3.0   |
| F5036         | 0.389     | -1208                 | -1325                 | +122  | + 45 | -      | + 68   | -0.8   |
| F5040         | 0.512     | -1276                 | -1448                 | + 1   | - 76 | - 76   | - 89   | -3.4   |
| F5044         | 0.615     | -1330                 | -1447                 | - 40  | -152 | - 73   | -141   | +0.4   |
| F5048         | 0.743     | -1364                 | -1530                 | - 30  | -190 | -140:  | -161   | -4.4   |
| F5053         | 0.893     | -1558                 | -                     | + 89  | -133 | - 68   | - 59   | -0.6   |
| F5057         | 0.001     | -1376                 | -                     | +195  | - 59 | - 20:  | + 41   | -3.2   |
| F5060         | 0.152     | -                     | -                     | +300: | + 79 | + 75   | +223   | -2.5   |
| F5065         | 0.276     | -1174                 | -1512:                | +226  | + 92 | + 80:  | +135   | -5.4   |
| F5069         | 0.386     | -1362                 | -1379::               | +131  | + 28 | + 88   | + 60   | -2.6   |
| F5070         | 0.508     | -1326                 | -1477                 | + 5   | - 49 | - 35   | - 32   | +0.4   |
| F5077         | 0.630     | -1280                 | -1495                 | - 56  | -163 | -142   | -215:  | -5.1   |
| F5081         | 0.754     | -1520                 | -1788:                | - 4   | -210 | -191   | -157:  | +0.5   |
| F5086         | 0.910     | -1468:                | -1508                 | +100  | -134 | -171:  | - 60   | -2.3   |
|               | HD 156385 |                       |                       |       |      |        |        |        |
| G8113         | -         | -1879                 | -                     | + 27: | -226 | - 16:  | -      | -2.0   |
| G8247         | -         | -1824                 | -                     | + 29: | -260 | + 45:: | -      | -4.3   |
| G8288         | -         | -1886                 | -                     | + 23  | -222 | - 60:  | -      | -2.6   |
| G8314         | -         | -1881                 | -                     | + 35  | -244 | -106:  | -      | +2.4   |

<sup>a</sup>The phase ephemerides are calculated using the final elements in Table 7.

star are more severe (cf. the case of the WC6, 18<sup>d</sup>4 binary O Mus: Moffat and Seggewiss 1977). Since the C IV emission lines 4441 and 4786 Å are of higher EP, we adopt their weighted mean semiamplitude as most appropriate for the orbit of the WC7 component:  $K(W) = 144 \pm 4 \text{ km s}^{-1}$ . Since these same lines yield essentially circular orbits, we now adopt  $e = 0$  as final. Due to systematic emission-line shifts and the lack of precise wavelengths, we defer finding the  $\gamma$  velocity to the discussion of the absorption lines of the O star.

For the photospheric absorption lines of the O star, adoption of a circular orbit and the above period yields the parameters of Table 6. The best semiamplitude is

obtained for those absorption lines which are superposed on a *straight* continuum. This is the case for H $\beta$ ,  $\gamma$ ,  $\delta$ , and He I 4471 which yield a weighted mean:  $K(O) = 84.6 \pm 1.3 \text{ km s}^{-1}$ . These lines are also used to define the final mean epoch of phases:  $E = \text{JD } 2,442,463.34 \pm 0.01$ . The K-values of the remaining lines are shifted in the expected sense, on the basis of the degree and sense of curvature of the underlying continuum. The most reliable  $\gamma$  velocity is obtained for He I 4471 which is superposed on the *flattest* continuum and has the most consistent value for CTIO and ESO (H8 is a close second choice, but it shows a curious phase-shift and is omitted); this we adopt for the system as a whole:  $\gamma = -10 \pm 8 \text{ km s}^{-1}$ .

TABLE 4  
HELIOCENTRIC RADIAL VELOCITIES ( $\text{km s}^{-1}$ ) FOR THE BEST  
ABSORPTION LINES OF THE O7 V COMPONENT OF HD 97152

| Ion :         | H $\beta$ | H $\gamma$ | H $\delta$ | H8    | H9    | HeI   | HeI   | HeII  |
|---------------|-----------|------------|------------|-------|-------|-------|-------|-------|
| $\lambda_o$ : | 4861      | 4340       | 4101       | 3889  | 3835  | 4026  | 4471  | 4541  |
|               | .332      | .468       | .737       | .051  | .386  | .19   | .48   | .590  |
| Plate         | phase     |            |            |       |       |       |       |       |
| A4106         | 0.212     | -          | -          | -117  | + 82  | -     | -     | -     |
| A4111         | 0.443     | -          | + 74:      | - 78: | -     | -     | -100: | - 79: |
| A4112         | 0.452     | -          | +112       | -139: | -     | -     | +161  | -139: |
| A4116         | 0.584     | -          | + 59       | - 6:  | + 71  | -     | +100: | -     |
| A4119         | 0.706     | -          | -          | + 77  | +104  | +121  | +108  | -     |
| A4123         | 0.831     | -          | + 96:      | + 75  | + 58  | + 98  | 0     | - 15: |
| A4424         | 0.832     | -          | +216:      | - 10  | + 99  | -     | -     | +105: |
| A4428         | 0.941     | -          | +144       | + 76  | +206  | +126  | +217  | + 48: |
| A4433         | 0.078     | -          | +158:      | + 53  | + 46  | + 19  | -     | + 58  |
| A4439         | 0.206     | -          | + 56       | - 62  | -     | -     | - 46: | - 91: |
| A4443         | 0.323     | -          | -          | - 92: | -105  | -     | -273: | - 29  |
| C4754         | 0.288     | -          | - 65:      | -264: | -102  | -233: | -108  | - 27: |
| C4804         | 0.640     | -          | + 44       | - 40  | + 78  | + 61  | - 75: | + 21  |
| C4810         | 0.769     | +113       | + 93:      | + 21  | + 41  | + 33  | + 45  | -     |
| C4824         | 0.884     | + 58       | +132       | - 1   | -     | -     | - 33  | + 19  |
| F5014         | 0.017     | -          | -          | -130  | -152  | + 36  | - 74: | -107  |
| F5023         | 0.134     | - 53       | -          | -160  | -127  | -     | -103  | - 35  |
| F5031         | 0.266     | - 46       | -          | - 87  | -122  | -     | -191  | - 91  |
| F5036         | 0.389     | + 62:      | -          | -154  | + 16  | -     | -134  | - 87  |
| F5040         | 0.512     | - 17       | -          | - 87  | + 33  | + 57  | - 46  | + 9   |
| F5044         | 0.615     | + 36       | -          | -115  | + 59  | + 39  | +141  | +103  |
| F5048         | 0.743     | +103       | -          | - 40  | - 16  | +112  | + 49  | -     |
| F5053         | 0.893     | -          | -          | - 25  | - 4   | +193  | -     | + 28  |
| F5057         | 0.001     | -          | -          | - 86  | -114: | + 70  | + 34  | - 31  |
| F5060         | 0.152     | - 42       | -          | -140  | -159  | -175  | -233  | - 62  |
| F5065         | 0.276     | -121       | -          | -181  | - 83  | -     | -106  | - 70  |
| F5069         | 0.386     | - 70       | -          | -160  | 0     | + 36  | - 71  | + 55  |
| F5070         | 0.508     | + 46       | -          | - 96  | + 80: | -     | - 23  | + 28  |
| F5077         | 0.630     | + 63       | -          | + 1   | + 33  | +119  | + 86  | + 22: |
| F5081         | 0.754     | + 33       | -          | + 10  | + 78  | +134  | + 6   | + 93  |
| F5086         | 0.910     | +132       | -          | - 45  | - 43  | +124  | + 37  | + 5   |

TABLE 5  
DERIVED PARAMETERS FOR EMISSION LINES OF WC7 COMPONENT HD 97152

| Parameter                                       | C III(iv) e        | He II e            | C IV e             | C IV e             |
|---|--------------------|--------------------|--------------------|--------------------|
| $\lambda_o(\text{\AA})$ : .....                 | 4650               | 4685               | 4441               | 4786               |
|   | ...                | 0.682              | ...                | ...                |
| $\chi(\text{eV})^a$ .....                       | 41(58)             | 51                 | 58                 | 58                 |
| $\gamma(\text{CTIO})(\text{km s}^{-1})$ .....   | $+95 \pm 13$       | $0 \pm 20$         | $-46 \pm 8$        | ...                |
| $\gamma(\text{ESO})(\text{km s}^{-1})$ .....    | $+107 \pm 2$       | $+8 \pm 8$         | $-55 \pm 3$        | $-22 \pm 11$       |
| $K(\text{km s}^{-1})$ .....                     | $160 \pm 3$        | $180 \pm 11$       | $143 \pm 4$        | $149 \pm 16$       |
| $\Delta\phi^b$ .....                            | $-0.098 \pm 0.003$ | $-0.056 \pm 0.009$ | $-0.010 \pm 0.004$ | $-0.003 \pm 0.016$ |
| $e$ .....                                       | $0.050 \pm 0.017$  | $0.095 \pm 0.057$  | $0.027 \pm 0.026$  | $0.077 \pm 0.105$  |
| $\omega(^{\circ})$ .....                        | $62 \pm 22$        | $307 \pm 34$       | $5 \pm 62$         | $315 \pm 80$       |
| disp. <sup>c</sup> (CTIO)( $\text{km s}^{-1}$ ) | 40                 | 73                 | 74                 | ...                |
| disp. <sup>c</sup> (ESO)( $\text{km s}^{-1}$ )  | 9                  | 25                 | 16                 | 35                 |

<sup>a</sup>  $\chi$  is the maximum of ionization potential of the preceding ion and upper excitation potential relative to the ground state of the ion.

<sup>b</sup>  $\Delta\phi = (E_{\text{line}} - E_{\text{H}\delta})/P$ ;  $E_{\text{H}\delta} = \text{JD } 2,442,463.42$ .

<sup>c</sup> disp. is defined here simply as the rms of the residual velocities.

TABLE 6  
DERIVED PARAMETERS FOR THE O STAR ABSORPTION LINES

| Parameter                       | H $\beta$          | H $\gamma$         | H $\delta$        | H9                 | He I<br>4026       | He I<br>4471       | He II<br>4541      |
|---------------------------------|--------------------|--------------------|-------------------|--------------------|--------------------|--------------------|--------------------|
| $\gamma$ (CTIO) .....           | +4 $\pm$ 30        | +57 $\pm$ 24       | -51 $\pm$ 10      | -54 $\pm$ 28       | -50 $\pm$ 25       | -7 $\pm$ 18        | -109 $\pm$ 12      |
| $\gamma$ (ESO) .....            | +11 $\pm$ 11       | ...                | -98 $\pm$ 7       | +30 $\pm$ 20       | -36 $\pm$ 12       | -10 $\pm$ 8        | -68 $\pm$ 18       |
| $K$ (km s <sup>-1</sup> ) ..... | 89 $\pm$ 15        | 81 $\pm$ 36        | 88 $\pm$ 9        | 137 $\pm$ 23       | 119 $\pm$ 16       | 77 $\pm$ 11        | 170 $\pm$ 15       |
| $\Delta\phi$ .....              | +0.031 $\pm$ 0.029 | -0.073 $\pm$ 0.048 | 0.000 $\pm$ 0.014 | -0.007 $\pm$ 0.026 | -0.038 $\pm$ 0.022 | -0.052 $\pm$ 0.022 | -0.046 $\pm$ 0.012 |
| disp. (CTIO) .....              | 21                 | 53                 | 48                | 46                 | 88                 | 69                 | 27                 |
| disp. (ESO) .....               | 47                 | ...                | 35                | 58                 | 52                 | 40                 | 92                 |

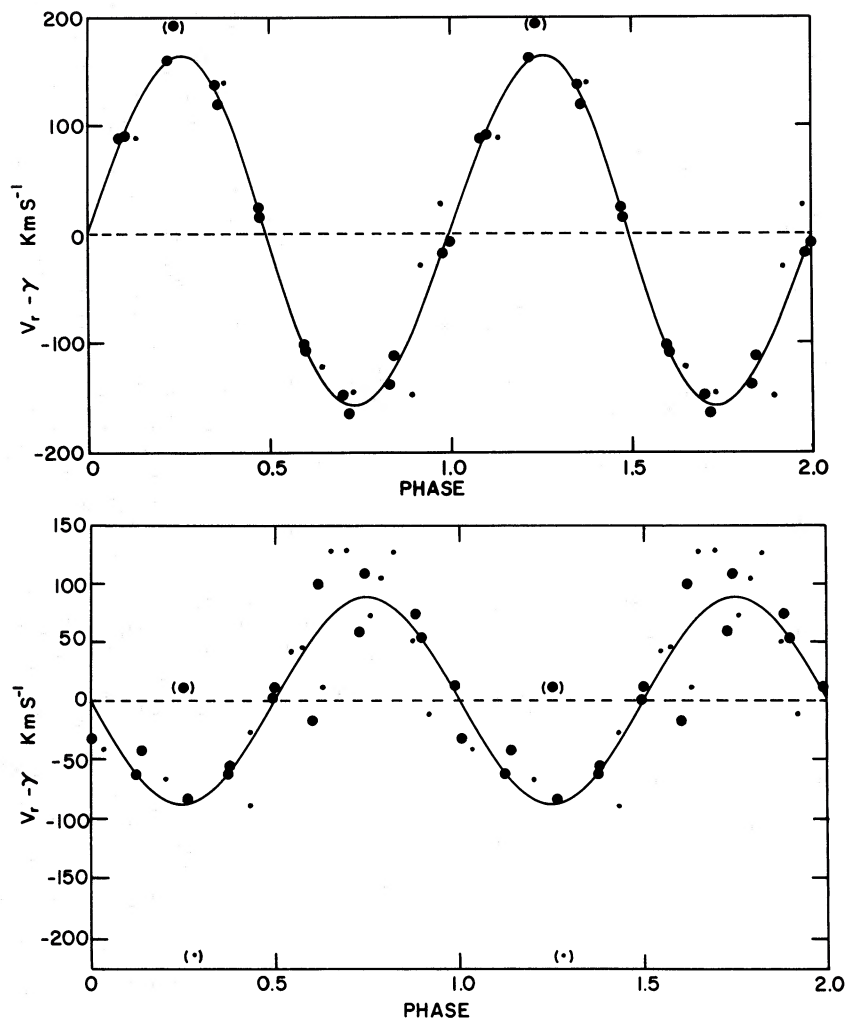


FIG. 3a, b.—Radial velocity ( $\gamma$  subtracted off) vs. phase, based on the elements of Tables 5 and 6, respectively, for C III(IV) 4650 emission and H $\delta$  absorption of HD 97152. Large dots refer to ESO data, small dots to CTIO. Data points whose observed radial velocities deviated from their calculated ones by more than  $2\sigma$  within their own group were not retained for the final fit; they are bracketed in the phase diagram.

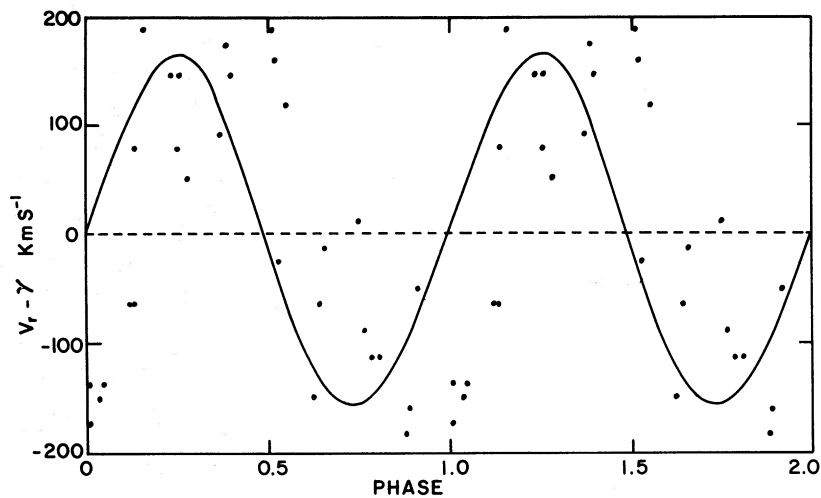


FIG. 4.—Radial velocity versus phase for the 4680 photometric data of Table 1. The curve refers to the orbit of C III(IV) *e* 4650 in Table 5.

TABLE 7

SUMMARY OF THE ELEMENTS ADOPTED

|          |                                      |
|----------|--------------------------------------|
| $P$      | $= 7^d886 \pm 0^d003$                |
| $e$      | $= 0.00$ (adopted)                   |
| $E$      | $= \text{JD } 2,442,463.34 \pm 0.01$ |
| $\gamma$ | $= -10 \pm 8 \text{ km s}^{-1}$      |
| $K(W)$   | $= 144 \pm 4 \text{ km s}^{-1}$      |
| $K(O)$   | $= 84.6 \pm 1.3 \text{ km s}^{-1}$   |

Again, the shift in  $\gamma$  values for the other lines is in the expected sense, according to the slope of the underlying continuum.

Finally, we summarize in Table 7 the adopted elements. From these we obtain the separation of the two stars:

$$a \sin i = \frac{P}{2\pi} (1 - e^2)^{1/2} [K(O) + K(W)] \\ = 35.8 \pm 0.7 R_{\odot},$$

compared with a probable radius of the O7 V star (Allen 1973),  $R(O) = 15 R_{\odot}$  and a probable radius of the core of the WC7 star (Rublev 1975),  $R_c(W) = 4-5 R_{\odot}$ . For the slightly cooler WC8 star  $\gamma^2$  Vel the radius of the 4650 Å emitting region is  $R_e(W) \approx 0.25 a = 74 R_{\odot}$  using angular diameter measurements of Hanbury-Brown *et al.* (1970), and the orbital elements of Niemela and Sahade (1980), and parallax by Conti and Smith (1972). This probably represents an upper limit for HD 97152 which is hotter and thus probably smaller, assuming similar luminosities, and it may be more realistic to take  $R_e \approx 5 R_c$  (Underhill 1969), that is, 20–25  $R_{\odot}$ .

From the ratio

$$M(W)/M(O) = K(O)/K(W)$$

and the mass function

$$[M(O) \sin i]^3 / [M(O) + M(W)]^2 \\ = (1 - e^2)^{3/2} P \times K(W)^3 / 2\pi G,$$

we get

$$M(W) \sin^3 i = 3.6 \pm 0.3 M_{\odot}$$

$$M(O) \sin^3 i = 6.1 \pm 0.5 M_{\odot}.$$

Weak constraints on the orbital inclination can be obtained from the lack of occultation phenomena in the light curves:

$$a \cos i > R(W) + R(O).$$

Taking  $R(W) = R_c(W)$  and  $a \sin i$  from above, one finds  $i < 62^\circ$ , thus implying

$$M(W) > 5.2 M_{\odot}$$

$$M(O) > 8.8 M_{\odot}.$$

Similar values arise if one assumes a canonical value  $i = 57^\circ$  based on random distribution of inclinations.

With  $R(W) = R_e(W) = 25 R_{\odot}$ , one finds  $i \lesssim 44^\circ$  which leads to

$$M(W) > 10.7 M_{\odot}$$

$$M(O) > 18.2 M_{\odot}.$$

Perhaps the best most reasonable estimate of the WR mass is reached by assuming a normal mass for the O7 V component of  $\sim 29 M_{\odot}$  (Allen 1973). This gives  $i = 36:5$  and  $M(W) = 17.5 M_{\odot}$ . Also, this yields  $a = 60 R_{\odot}$ , implying that part of the WR envelope may indeed extend beyond the system as a whole. This is compatible with the radial velocity variations of the P Cygni absorption edges of He I 3888 and C III(IV) 4650 (Fig. 5), which are formed near the outer extremities of the envelope. The variation is strongly phase-shifted and distorted compared with the C IV emission lines, likely a result of perturbation from both stars.

## VI. FINAL REMARKS

Although its position in the Galaxy does not allow one to obtain a precise distance estimate using a galactic rotation model and its observed radial velocity, it is useful to reverse the problem and make a consistency check. Taking the solar galactocentric distance  $R_0 = 8.5 \pm 0.5$  kpc and constant rotation velocity near the solar circle  $\theta_0 = 220 \pm 10 \text{ km s}^{-1}$  (Gunn, Knapp, and Tremaine 1979), we find the expected net radial component of galactic rotation  $V_{\text{LSR}}(\text{exp}) = \theta_0 \sin l (R_0/R - 1) = -14.5(+2.7; +0.6) \text{ km s}^{-1}$ , assuming our distance  $d$ , and  $R^2 = R_0^2 + d^2 - 2dR_0 \cos l$ . Thus,  $V_{\text{LSR}}$  is very insensitive to changes in distance in the range of interest and agrees well with the adopted value  $V_{\text{LSR}}(\text{obs}) = \gamma + u_0 \sin l + v_0 \cos l = -12 \pm 8 \text{ km s}^{-1}$ , where  $u_0 = 7.4$ ,  $v_0 = 10 \text{ km s}^{-1}$  for B stars (Balona and Feast 1974).

From the present observations, the most accurate quantity obtained is probably the mass ratio  $M(W)/M(O) = 0.59 \pm 0.02$ . The other three known WC binaries yield a mean ratio  $0.38 \pm 0.09$  (s.e.m.), while the eight known WN binaries give  $0.44 \pm 0.08$  (s.e.m.). Including the present value, the WC ratio becomes  $0.43 \pm 0.08$  (s.e.m.), which is similar to the WN ratio. Assuming the OB companions to have similar masses in the mean, this implies that WN stars lose little mass when they evolve into WC stars, if that is indeed what happens (cf. Moffat and Seggewiss 1980). In any case, the ratios are compatible with the general hypothesis that WR stars, originally the more massive stars in these binaries, represent the cores of massive supergiants which have lost their outer, more tenuous layers probably by a combination of mass transfer and stellar wind mass loss.

Concerning the individual masses, if the O7 V companion is not undermassive for its luminosity, the WC7 component has a mass  $M(\text{WC7}) = 17.5 M_{\odot}$ . This is close to the lower limit ( $i = 90^\circ$ ) for the WC8 component of  $\gamma^2$  Vel (Niemela and Sahade 1980) who find  $M(\text{WC8}) \geq 17 M_{\odot}$ . For the other WC + OB binaries (Moffat and Seggewiss 1980) the limits are lower, possibly a result of relatively low orbital inclination.

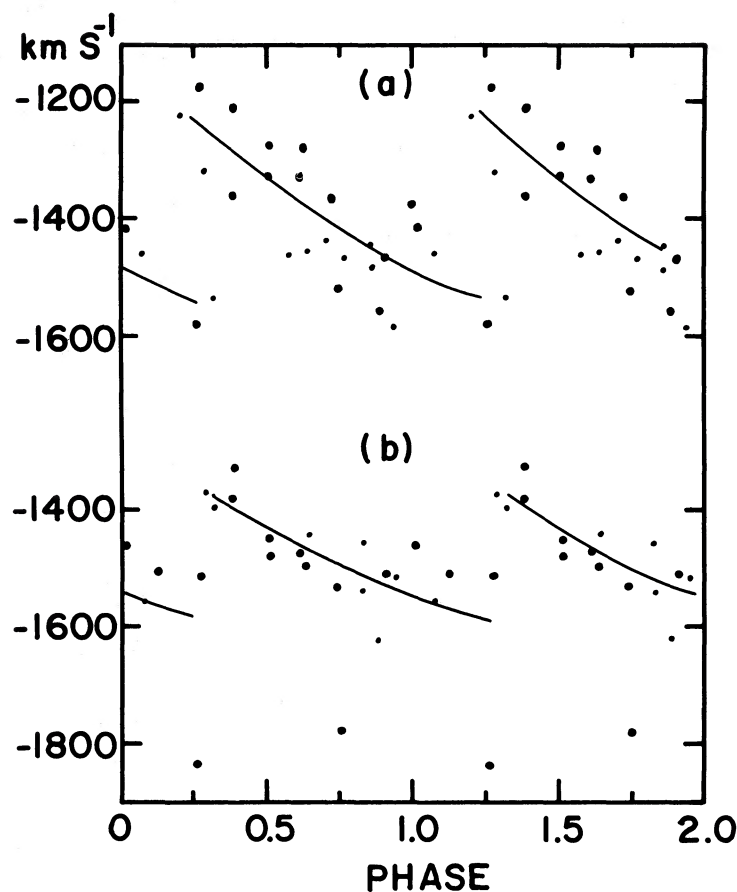


FIG. 5.—Radial velocity versus phase (Table 7) for the P Cygni type violet absorption edges of (a) He I 3888 and (b) C III(IV) 4650 of HD 97152. Symbols as in Fig. 3. As in Figs. 3 and 4, the WR component is in front at phase zero.

Before a meaningful comparison is made with theoretical evolutionary scenarios for advanced stages of massive binaries, we consider it essential first to gather more spectroscopic and photometric data for other WR stars. Systematic programs to do this are in progress for WR stars spanning the whole Milky Way as well as the Magellanic Clouds.

A.F.J.M. is grateful to Th. Schmidt-Kaler for observing time on the 61 cm Bochum telescope in Chile; to the

European Southern Observatory for a generous allotment of observing time; and to C. T. Bolton and R. Lyons for measuring time and assistance on the PDS at the David Dunlap Observatory. Financial assistance to A.F.J.M. came from the Comité d'Attribution des Fonds Internes de Recherches of the Université de Montréal and the National Research Council of Canada. V.S.N. is obliged to the Director of CTIO, V. Blanco, for the use of the Observatory facilities.

#### REFERENCES

- Allen, C. W. 1973, *Astrophysical Quantities* (London: Athlone Press).  
 Balona, L. A., and Feast, M. W. 1974, *M.N.R.A.S.*, **167**, 621.  
 Conti, P. S., and Alschuler, W. R. 1971, *Ap. J.*, **170**, 325.  
 Conti, P. S. and Smith, L. F. 1972, *Ap. J.*, **172**, 623.  
 Cruz-González, C., Recillas-Cruz, E., Costero, R., Peimbert, M., and Torres-Peimbert, S. 1974, *Rev. Mexicana Astr. Ap.*, **1**, 211.  
 Gunn, J. E., Knapp, G. R., and Tremaine, S. P. 1979, *A.J.*, **84**, 1181.  
 Hanbury-Brown, R., Davis, J., Herbison Evans, D., and Allen, L. R. 1970, *M.N.R.A.S.*, **148**, 103.  
 Lafer, J., and Kinman, T. D. 1965, *Ap. J. Suppl.*, **11**, 216.  
 Moffat, A. F. J. 1977, *Inf. Bull. Var. Stars*, No. 1265.  
 ———. 1978, *Astr. Ap.*, **68**, 41.  
 Moffat, A. F. J. and Seggewiss, W. 1977, *Astr. Ap.*, **54**, 607.  
 ———. 1980, in *IAU Symposium No. 88, Close Binary Stars: Observation and Interpretation*, ed. M. Plavec and R. K. Ulrich (Dordrecht: Reidel), p. 181.  
 Niemela, V. S., and Sahade, J. 1980, *Ap. J.*, **238**, 244.  
 Roberts, M. S. 1962, *A.J.*, **67**, 79.  
 Rublev, S. 1975, in *IAU Symposium No. 67, Variable Stars and Stellar Evolution*, ed. V. E. Sherwood and L. Plaut (Dordrecht: Reidel), p. 259.  
 Smith, L. F. 1968a, *M.N.R.A.S.*, **138**, 109.  
 ———. 1968b, *M.N.R.A.S.*, **140**, 409.  
 ———. 1968c, *M.N.R.A.S.*, **141**, 317.

———. 1973, in *IAU Symposium No. 49, Wolf-Rayet and High Temperature Stars*, ed. M. K. V. Bappu and J. Sahade (Dordrecht: Reidel), p. 15.

Turner, D. G. 1980, *Pub. A.S.P.*, in press.

Underhill, A. B. 1969, in *Mass Loss from Stars*, ed. M. Hack (Dordrecht: Reidel), p. 17.

Vogt, N., and Moffat, A. F. J. 1975, *Astr. Ap.*, **39**, 477.

ANTHONY B. DAVIS and ANTHONY F. J. MOFFAT: Département de physique, Université de Montréal, C.P. 6128, Succ. A., Montréal, Que., H3C 3J7, Canada

VIRPI S. NIEMELA: Instituto de Astronomia y Fisica del Espacio, Casilla de Correo 67, Suc. 28, 1428 Buenos Aires, Argentina